Respiratory effects of the scalene and sternomastoid muscles in humans

Alexandre Legrand, Emmanuelle Schneider, Pierre-Alain Gevenois and André De Troyer

---

You might find this additional info useful...

This article cites 23 articles, 17 of which you can access for free at:
http://jap.physiology.org/content/94/4/1467.full#ref-list-1

This article has been cited by 9 other HighWire-hosted articles:
http://jap.physiology.org/content/94/4/1467#cited-by

Updated information and services including high resolution figures, can be found at:
http://jap.physiology.org/content/94/4/1467.full

Additional material and information about *Journal of Applied Physiology* can be found at:
http://www.the-aps.org/publications/jappl

This information is current as of January 12, 2013.

Respiratory effects of the scalene and sternomastoid muscles in humans

**Alexandre Legrand, Emmanuelle Schneider,
Pierre-Alain Gevenois, and André De Troyer**
*Laboratory of Cardiorespiratory Physiology, Brussels School of Medicine, and Chest Service
and Department of Radiology, Erasme University Hospital, 1070 Brussels, Belgium*

Legrand, Alexandre, Emmanuelle Schneider, Pierre-Alain Gevenois, and André De Troyer. Respiratory effects of the scalene and sternomastoid muscles in humans. *J Appl Physiol* 94: 1467–1472, 2003; 10.1152/japplphysiol.00869. 2002.—Previous studies have shown that in normal humans the change in airway opening pressure (ΔPao) produced by all the parasternal and external intercostal muscles during a maximal contraction is approximately -18 cmH$_2$O. This value is substantially less negative than ΔPao values recorded during maximal static inspiratory efforts in subjects with complete diaphragmatic paralysis. In the present study, therefore, the respiratory effects of the two prominent inspiratory muscles of the neck, the sternomastoids and the scalenes, were evaluated by application of the Maxwell reciprocity theorem. Seven healthy subjects were placed in a computed tomographic scanner to determine the fractional changes in muscle length during inflation from functional residual capacity to total lung capacity and the masses of the muscles. Inflation induced greater shortening of the scalenes than the sternomastoids in every subject. The inspiratory mechanical advantage of the scalenes thus averaged (mean $\pm$ SE) $3.4 \pm 0.4\%$/l, whereas that of the sternomastoids was $2.0 \pm 0.3\%$/l ($P < 0.001$). However, sternomastoid muscle mass was much larger than scalene muscle mass. As a result, ΔPao generated by a maximal contraction of either muscle would be 3–4 cmH$_2$O, which is about the same as ΔPao generated by the parasternal intercostals in all interspaces.

respiratory muscles; mechanics of breathing; muscles of the neck

---

ALTHOUGH THE ACTIONS of most respiratory muscles on the chest wall and the lung in humans have been qualitatively described, the amount of lung expansion (or deflation) a particular muscle can produce has not been determined. This is a difficult problem, because many muscles are inaccessible and cannot be maximally activated in isolation. However, theoretical studies by Wilson and De Troyer (22, 23) have proposed an indirect approach based on the Maxwell reciprocity theorem. When applied to the respiratory system, this standard theorem of mechanics predicts that the respiratory effect of a given muscle [i.e., change in airway opening pressure (ΔPao) produced by the muscle during a maximal isolated contraction against a closed airway] is related to the mass (m) of the muscle, the maximal active muscle tension per unit cross-sectional area (σ), and the fractional change in muscle length (ΔL) per unit volume increase of the relaxed chest wall [$(L/\Delta V_L)_{Rel}$], such that

$$\Delta \text{Pao} = m\sigma \left[\Delta L(L/\Delta V_L)_{Rel}\right] \qquad (1)$$

In agreement with *Eq. 1*, a number of studies in dogs have demonstrated that a muscle that shortens during passive inflation does cause a fall in Pao when it contracts alone (11, 19). Conversely, a muscle that lengthens during passive inflation causes a rise in Pao during contraction (9). In addition, the coefficient of proportionality (σ) between ΔPao per unit muscle mass and $\Delta L(L/\Delta V_L)_{Rel}$ was the same for all the muscles and amounted to 3.0 kg/cm^2. Therefore, it was concluded that the respiratory effect of a particular muscle can indeed be estimated simply by measuring its mass and its fractional change in length during passive inflation, and this principle was then used to evaluate the respiratory effects of the inspiratory intercostal muscles in humans. The total pressure generated by a maximal contraction of the parasternal intercostals in all interspaces was -3 cmH$_2$O (10), and that generated by the external intercostals in all interspaces was -15 cmH$_2$O (24). Consequently, the magnitude of the ΔPao generated by the parasternal and external intercostal muscles contracting maximally and simultaneously would amount to approximately -18 cmH$_2$O.

However, measurements of respiratory muscle strength in subjects with complete diaphragmatic paralysis have shown that the ΔPao values developed by such subjects during maximal static inspiratory efforts are substantially more negative, averaging -30 cmH$_2$O (2, 16). This difference suggests that a chronic paralysis of the diaphragm induces hypertrophy of the inspiratory intercostals and, thereby, enhances their pressure-generating ability. Alternatively, or additionally, a substantial proportion of the pressure developed by these subjects would be generated by muscles other than the parasternal and external intercostals. In the present study, therefore, we have assessed the respiratory ef-

Address for reprint requests and other correspondence: A. De Troyer, Chest Service, Erasme University Hospital, 808 Route de Lennik, 1070 Brussels, Belgium (E-mail: a_detroyer@yahoo.fr).

fects of the two most prominent inspiratory muscles in the neck, the scalenes and the sternomastoids.

METHODS

The studies were performed in seven healthy subjects (5 men and 2 women) 29–49 yr of age. The subjects had normal pulmonary function tests, and their principal anthropometric characteristics and supine inspiratory capacity are listed in Table 1. They gave informed consent to the procedures, which conformed with the Declaration of Helsinki and were approved by the Ethics Committee of the Brussels School of Medicine. Five subjects had previously participated in many respiratory experiments and were highly trained in relaxing their respiratory muscles at different lung volumes, but two subjects (*subjects 5* and *7*) had little prior experience as respiratory subjects. Before the study, these two subjects underwent several practice sessions with pairs of respiratory magnetometers (Norman H. Peterson, Boston, MA) placed on the abdomen and rib cage, during which they were coached to relax their respiratory muscles. At the time of the study, all subjects were able to produce consistent relaxation curves of the chest wall from resting end expiration [functional residual capacity (FRC)] to total lung capacity (TLC).

On the day of the study, the subject was placed supine in a computed tomographic (CT) scanner (Somaton Plus 4A, Siemens Medical System, Forschheim, Germany), and all restrictive garments were removed. Once positioned, the subject hyperventilated for 10–20 s and held his or her breath at FRC for 25 s, at which time spiral data were acquired starting 1 cm cranial to the mastoid process and extending to 1 cm caudal to the ventral part of the second rib. The scanning parameters were 140 kV, 206 mA, 1.0 s per revolution scanning time, 3 mm collimation, and 4 mm/s table feed. The subject then breathed in up to TLC and relaxed the respiratory muscles with the glottis closed, and a second set of spiral data was acquired. After this procedure was completed, transverse CT scans at FRC and TLC were reconstructed at 2.5-mm intervals by using a 360° linear interpolation algorithm and a standard kernel; depending on the subject's height, a total of 80–110 successive transverse images were thus obtained at each lung volume. Sagittal and coronal images were also reconstructed, and these multiplanar reformations of the neck were then used in a display workstation (Virtuoso, Siemens Medical System) to measure the fractional changes in sternomastoid and scalene muscle length during passive inflation as well as the masses of the muscles.

Changes in muscle length. Sternomastoid muscle length on both sides of the neck was first measured at FRC (Fig. 1). The point corresponding to the caudal edge of the mastoid process was carefully defined (Fig. 1A), and the three-dimensional coordinates of this point were recorded. By using the sagittal

(Fig. 1B) and coronal (Fig. 1C) images, the muscle from this point was then followed in the caudal and ventral directions to the manubrium sterni. The three-dimensional coordinates of the cranial edge of the manubrium were also recorded (Fig. 1C), and the linear distance between the two points, representing the length of the sternal head of the muscle at FRC, was computed (Fig. 1D). The length of the clavicular head of the sternomastoid at FRC was similarly obtained by measuring the linear distance between the caudal edge of the mastoid process and the muscle insertion on the clavicle. The distances between these pairs of points in their positions at TLC were subsequently measured by using the same procedure, and the fractional changes in length of the two heads of the sternomastoid were calculated from the differences between the distances at FRC and TLC.

The changes in scalene muscle length were also evaluated in each subject by measuring the linear distances between the cranial and caudal bony insertions of the different muscle heads at FRC and TLC. Thus, at each lung volume, the anterior head, middle head, and posterior head of the muscle were identified on the transverse CT images just cranial to the first and second ribs, and each head was followed in the cranial direction to its origins on the transverse processes of the sixth, fifth, and fourth cervical vertebrae (C_6, C_5, and C_4, respectively). By using the reconstructed transverse, sagittal, and coronal CT images simultaneously, the points corresponding to the most lateral aspect of the three transverse processes were then defined, and their three-dimensional coordinates were recorded. The costal insertions of the muscle bundles originating from these three transverse processes were subsequently determined. The insertions on the first rib of the bundles making up the anterior head and the middle head of the muscle were easily visualized in every subject, such that the length of the C_4, C_5, and C_6 muscle bundles of the anterior and middle heads could be determined with precision. On the other hand, in some subjects, the point of insertion of the posterior head of the scalene on the second rib could not be seen clearly. The fractional changes in length of the posterior head, therefore, were not assessed.

Muscle mass. In each subject, each transverse CT image was also examined at window settings appropriate for displaying muscle structures (window width ~400 Hounsfield units, window level ~35 Hounsfield units), and the contours of the sternomastoid and scalene muscles were traced on the right and left sides of the neck for computation of their cross-sectional area. The muscle mass corresponding to a particular image was then obtained by multiplying the cross-sectional area by the thickness of the slice (2.5 mm) and by muscle density (1.056 g/cm^3), and the total muscle mass was obtained by adding all the unitary masses.

In our previous studies of the respiratory effects of the interchondral (10) and interosseous (24) intercostal muscles, the distributions of muscle mass were determined in cadavers from elderly individuals. Indeed, the intercostal muscles in humans are smaller than the muscles studied here, and their mass cannot be accurately determined from CT images. To make a useful comparison between the respiratory effects of the intercostal muscles and those of the neck muscles and to evaluate the total respiratory effect of the inspiratory muscles of the rib cage compartment of the chest wall, it was therefore important to measure sternomastoid and scalene muscle mass in cadavers as well. Five cadavers without overt malnutrition, obesity, or other thoracic deformity were thus selected from the pool of human bodies in the Department of Anatomy of the Brussels School of Medicine, and in each of them, the sternomastoids and scalenes were exposed on both sides of the neck, harvested, and weighed.

Table 1. *Characteristics of the subjects*

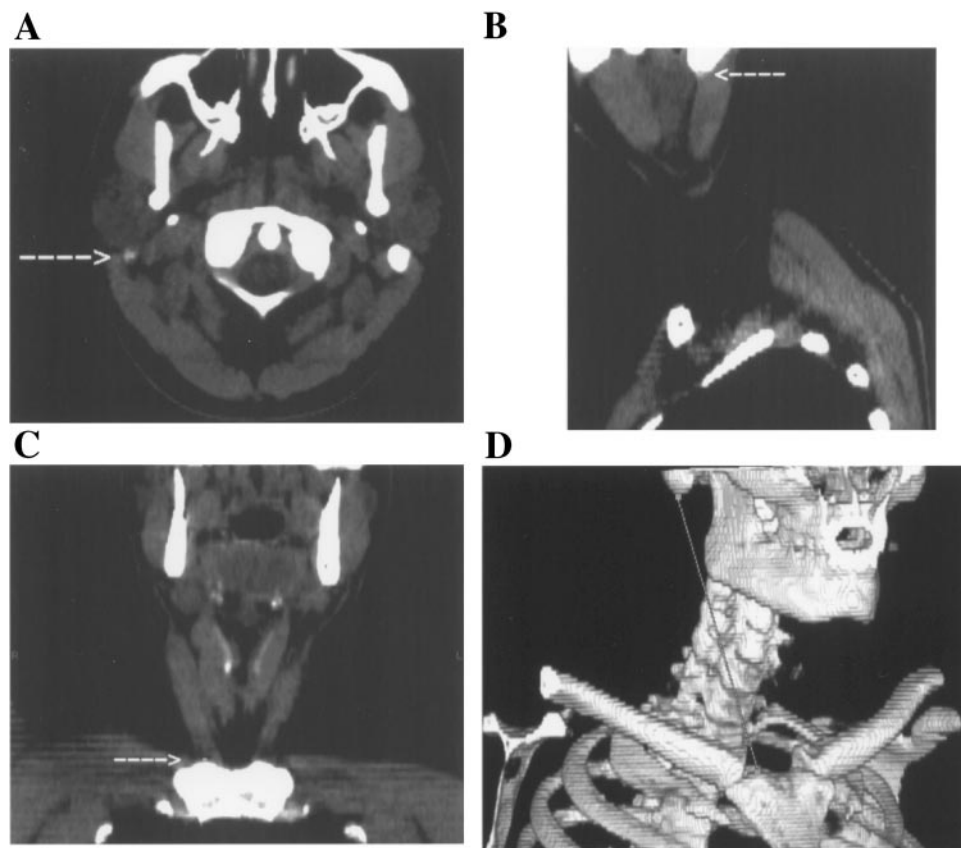| Sub No.	Gender	Age, yr	Height, cm	Weight, kg	Inspiratory Capacity, liters
1	M	43	177	65	3.65
2	M	47	192	77	4.04
3	F	48	150	42	2.10
4	M	38	170	60	4.65
5	M	37	182	80	3.95
6	M	49	180	77	3.85
7	F	29	169	58	3.20

Fig. 1. Computed tomographic (CT) scan images of the neck in a healthy subject at functional residual capacity (FRC). *A*: reconstructed transverse image through the caudal edge of the right mastoid process (arrow). *B*: sagittal image showing the caudal edge of the mastoid process (arrow) and the cranial portion of the sternomastoid muscle. *C*: coronal image, with the caudal portion of the sternal head of the muscle and its insertion on the cranial edge of the manubrium sterni (arrow). *D*: 3-dimensional view of the neck. Line connects the caudal edge of the right mastoid process to the cranial edge of the manubrium sterni; it corresponds, therefore, to the sternal head of the sternomastoid.

Data analysis. The muscles on the right and left sides of the neck did not show any systematic difference in mass or in fractional changes in length during passive inflation. Therefore, the fractional changes in muscle length on the two sides were averaged in each individual subject, and the muscle masses on the right side were added to those on the left side. These data were then averaged over the subject group and presented as means $\pm$ SE. Statistical comparisons between the length changes and the masses of the sternomastoids and scalenes were made by using paired *t*-tests. The criterion for statistical significance was taken as $P < 0.05$.

RESULTS

Changes in muscle length. The sternomastoid and scalene muscles were shorter during relaxation at TLC than at FRC in all subjects. Because the sternal head of the sternomastoid is longer than the clavicular head at FRC, its fractional shortening during inflation tended to be smaller. Similarly, fractional shortening tended to be greater in the scalene muscle bundles originating from the transverse processes of C_6 than in the longer muscle bundles originating from the transverse processes of C_4. However, these topographic differences were small. In addition, no differences were found between muscle bundles of the anterior head and the middle head of the scalene and originating from a given cervical segment. Consequently, the values of fractional shortening obtained for the two heads of the scalene were averaged, as were those obtained for the sternal and clavicular heads of the sternomastoid.

The values thus calculated for the two muscles in each individual subject are shown in Fig. 2. The scalenes consistently showed greater fractional shortening than the sternomastoids. For the seven subjects, whereas the shortening of the scalenes averaged
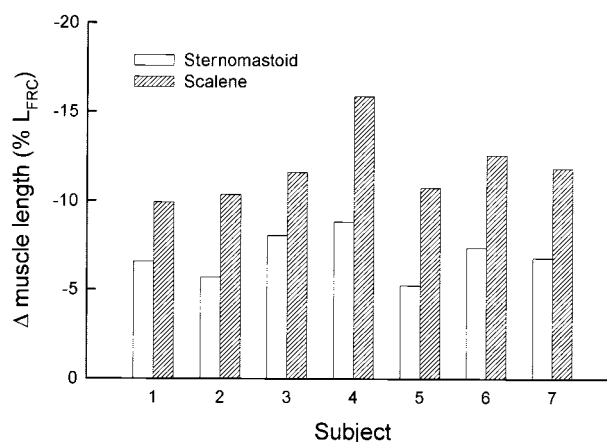

Fig. 2. Fractional changes in sternomastoid and scalene muscle length during inflation from FRC to total lung capacity (muscles relaxed) in 7 healthy subjects. Changes in sternomastoid muscle length are averages for the sternal head and the clavicular head of the muscle; changes in scalene muscle length are averages for muscle bundles originating from the transverse processes of C_4, C_5, and C_6 and making up the anterior head and the middle head of the muscle. Values are percent changes relative to muscle length at FRC (L_{FRC}).

11.84 ± 0.76%, the shortening of the sternomastoids was only 6.94 ± 0.48% ($P < 0.001$).

Muscle mass. Figure 3 shows bilateral sternomastoid and scalene muscle mass in the seven healthy subjects. Sternomastoid muscle mass averaged 110.1 ± 13.5 g, whereas scalene muscle mass was only 54.9 ± 6.2 g ($P < 0.001$). The two muscles showed a similar mass ratio in the cadavers. However, sternomastoid and scalene muscle masses in these subjects were only 62.4 ± 8.0 and 33.2 ± 3.2 g, respectively.

Computed mechanical advantages and respiratory effects. For a machine, such as a lever, "mechanical advantage" is defined as the ratio of the force delivered at the load to the force applied at the handle. By analogy, the mechanical advantage of a respiratory muscle may therefore be defined as $\Delta Pao/m\sigma$, which, according to *Eq. 1*, can be evaluated by measuring $\Delta L(L/\Delta V_L)_{Rel}$ (22, 23). Also, the maximum ΔPao that this muscle can produce can be calculated by multiplying mechanical advantage by muscle mass and maximum active stress. The mechanical advantages of the sternomastoid and scalene muscles in every subject of the study were thus obtained by dividing the fractional changes in muscle length by the inspiratory capacity, and these values were then multiplied by the corresponding values of muscle mass. Maximum active muscle stress was assumed to be similar to that of the dog (i.e., 3.0 kg/cm^2).

The results of these calculations are summarized in Fig. 4. As anticipated from the data shown in Fig. 2, the inspiratory mechanical advantage of the scalenes averaged 3.43 ± 0.38%/l and was invariably greater ($P < 0.001$) than that of the sternomastoid (2.05 ± 0.31%/l). However, because the mass of the sternomastoid was much greater (Fig. 3), the inspiratory effect of the muscle amounted to −6.27 ± 0.64 cmH$_2$O and was not significantly different from that of the scalenes (−5.35 ± 0.43 cmH$_2$O).

DISCUSSION

Electromyographic (EMG) recordings from the neck muscles in normal humans have established that the scalenes are invariably active during the inspiratory
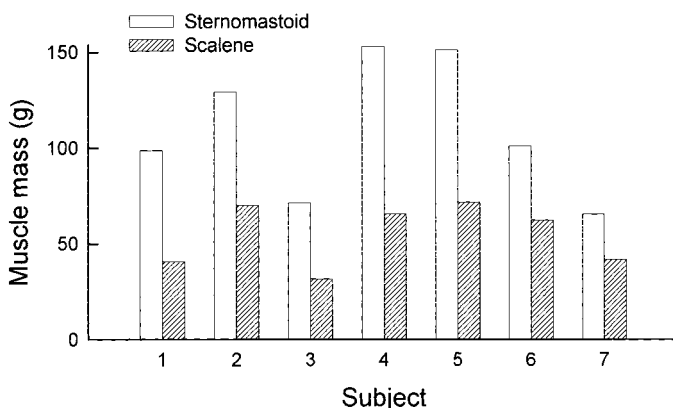

Fig. 3. Mass of sternomastoid and scalene muscles (both sides of the neck) in 7 healthy subjects.
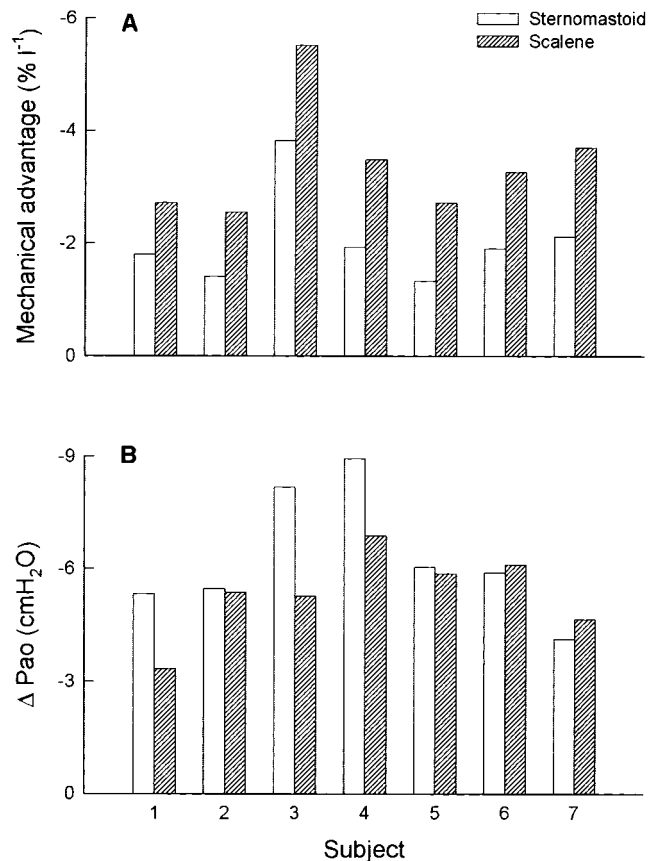

Fig. 4. Mechanical advantages (*A*) and respiratory effects (*B*) of sternomastoid and scalene muscles in 7 healthy subjects. Values of mechanical advantage were obtained by dividing fractional changes in muscle length during passive inflation by inspiratory capacity; a negative value indicates an inspiratory mechanical advantage. Values of respiratory effect are changes in airway opening pressure (Pao) generated by muscles during a maximal contraction against a closed airway; these values were computed by multiplying mechanical advantage by muscle mass and maximal active muscle stress (3.0 kg/cm^2).

phase of the breathing cycle, including when the increase in lung volume is very small (4, 13, 21). The sternomastoids are not active during resting breathing, but they do contract during strong inspiratory efforts, such as during a maximal lung inflation (1, 21). Also, when the scalenes or the sternomastoids in dogs are selectively stimulated by electrical activation, they induce a marked cranial displacement of the rib cage with an increase in the dorsoventral rib cage diameter and an increase in lung volume (7). In humans with tetraplegia due to transection of the upper cervical cord, which causes paralysis of the diaphragm, intercostal, and scalene muscles and leaves the sternomastoids intact, spontaneous contraction of the sternomastoids similarly produces a large cranial displacement of the rib cage and an inflation of the lung (3, 5). Together, these observations indicate that these two sets of muscles have inspiratory actions, so it was expected that both would be shorter at TLC than at FRC.

Recent EMG studies in dogs have also shown that the topographic distribution of neural drive among the

parasternal and external intercostals during breathing is closely matched to the distribution of inspiratory mechanical advantage, such that the muscle areas with the greatest mechanical advantage are also those that receive the greatest inspiratory drive (8, 17, 18). A similar matching between neural drive and mechanical advantage has also been demonstrated for the canine diaphragm (15) and the external intercostals in humans (6). Indeed, in humans breathing at rest in the seated posture, external intercostal inspiratory activity is greatest in the dorsal portion of the rostral interspaces, where the inspiratory mechanical advantage is greatest, and decreases gradually in the ventral and caudal directions, as does the mechanical advantage. As pointed out above, the scalenes in humans have a lower threshold of activation than the sternomastoids. Therefore, if this matching principle applied equally to the muscles of the neck, it would also be expected that inflation from FRC to TLC would be associated with greater fractional shortening of the scalenes.

In agreement with these predictions, inflation from FRC to TLC consistently elicited shortening of both muscles and caused greater fractional shortening of the scalenes (Fig. 2). Thus, as in the dog (19), both muscles in humans have an inspiratory mechanical advantage, and the scalenes have a greater mechanical advantage than the sternomastoids. However, the sternomastoids have a larger mass. As for the cadavers, sternomastoid muscle mass in every healthy subject of this study was about twice as large as scalene muscle mass (Fig. 3). As a result, the maximal ΔPao calculated for either muscle (Fig. 4B) amounted to -5 to 6 cmH_2O.

These estimates of maximal ΔPao are probably high for two reasons. First, studies on the human thigh have shown that CT measurements tend to overestimate cross-sectional areas of individual muscles by 10–20% (12). Second, the maximal ΔPao values thus calculated imply that both muscles can be maximally activated during inspiratory efforts, and this appears to be incorrect. Thus, using surface electrodes and intramuscular wire electrodes in normal subjects, Gandevia et al. (14) demonstrated that the amount of EMG activity recorded from the sternomastoids during maximal static inspiratory efforts is only 50% of that recorded during forceful rotations of the head. If one assumes that these postural maneuvers result in maximal sternomastoid activity, then one has to conclude that static inspiratory efforts involve maximal contraction of only half of the muscle fibers or, alternatively, that the effective tension per unit sternomastoid cross-sectional area during such efforts is only 50% of maximum, i.e., 1.5 kg/cm^2. In either case, the maximal ΔPao for the sternomastoids would be only -3.0 cmH_2O. Similarly, Gandevia et al. showed that the amount of EMG activity recorded from the scalenes during maximal static inspiratory efforts is 70% of the activity recorded during lateral flexion of the head. The maximal ΔPao for this muscle, therefore, should be only 0.7×-5.0 cmH_2O or -3.5 cmH_2O, and the total ΔPao produced by a maximal, simultaneous contraction of the scalenes and sternomastoids would amount to approximately -6.5 cmH_2O.

The mechanical advantages of the parasternal and external intercostal muscles in humans were previously computed by using CT images of the ribs and sternum similar to those used in the present study (10, 24). However, the values of intercostal muscle mass were obtained from measurements in cadavers from elderly, probably unfit, individuals, and the respiratory effects of the muscles were estimated by assuming that muscle mass in young healthy individuals would be twice that in cadavers. In the present study, the mass of the sternomastoids and scalenes in cadavers was about half that in healthy subjects. This confirmation is important, because it supports our previous results that the maximal inspiratory effects of the parasternal intercostals and external intercostals in humans amount, respectively, to approximately -3 and -15 cmH_2O. This confirmation also indicates that the inspiratory effect of the scalenes and sternomastoids together is $\sim$40% of the inspiratory effect of the external intercostals in all interspaces but twice as large as the effect of the parasternal intercostals.

We previously showed that in the dog the ΔPao produced by the simultaneous contraction of the scalenes and parasternal intercostals is, within 10%, equal to the sum of the ΔPao produced by the two sets of muscles individually (20). A similar finding was reported for the sternomastoids and parasternal intercostals (20), and there is no reason to believe that the interactions between these muscles in humans would be fundamentally different. On the basis of the ΔPao values derived from the present study and those previously computed for the parasternal and external intercostals (10, 24), it is reasonable to conclude that a forceful, simultaneous contraction of all the rib cage inspiratory muscles in normal humans would result in a ΔPao of approximately -25 cmH_2O. This value is still slightly less negative than the average pressure (i.e., -30 cmH_2O) measured during maximal static inspiratory efforts in subjects with complete diaphragmatic paralysis (2, 16), suggesting that such subjects indeed develop hypertrophy of the inspiratory intercostal and neck muscles.

REFERENCES

1. **Campbell EJM.** The role of the scalene and sternomastoid muscles in breathing in normal subjects. An electromyographic study. *J Anat* 89: 378–386, 1955.
2. **Celli BR, Rassulo J, and Corral R.** Ventilatory muscle dysfunction in patients with bilateral idiopathic diaphragmatic paralysis: reversal by intermittent external negative pressure ventilation. *Am Rev Respir Dis* 136: 1276–1278, 1987.
3. **Danon J, Druz WS, Goldberg NB, and Sharp JT.** Function of the isolated paced diaphragm and the cervical accessory muscles in C_1 quadriplegics. *Am Rev Respir Dis* 119: 909–919, 1979.
4. **De Troyer A and Estenne M.** Coordination between rib cage muscles and diaphragm during quiet breathing in humans. *J Appl Physiol* 57: 899–906, 1984.
5. **De Troyer A, Estenne M, and Vincken W.** Rib cage motion and muscle use in high tetraplegics. *Am Rev Respir Dis* 133: 1115–1119, 1986.

6. **De Troyer A, Gorman R, and Gandevia SC.** Distribution of inspiratory drive to the external intercostal muscles in humans. *J Physiol*. In press.

7. **De Troyer A and Kelly S.** Action of neck accessory muscles on rib cage in dogs. *J Appl Physiol* 56: 326–332, 1984.

8. **De Troyer A and Legrand A.** Inhomogeneous activation of the parasternal intercostals during breathing. *J Appl Physiol* 79: 55–62, 1995.

9. **De Troyer A and Legrand A.** Mechanical advantage of the canine triangularis sterni. *J Appl Physiol* 84: 562–568, 1998.

10. **De Troyer A, Legrand A, Gevenois PA, and Wilson TA.** Mechanical advantage of the human parasternal intercostal and triangularis sterni muscles. *J Physiol* 513: 915–925, 1998.

11. **De Troyer A, Legrand A, and Wilson TA.** Rostrocaudal gradient of mechanical advantage in the parasternal intercostal muscles of the dog. *J Physiol* 495: 239–246, 1996.

12. **Engstrom CM, Loeb GE, Reid JG, Forrest WJ, and Avruch L.** Morphometry of the human thigh muscles. A comparison between anatomical sections and computer tomographic and magnetic resonance images. *J Anat* 176: 139–156, 1991.

13. **Gandevia SC, Leeper JB, McKenzie DK, and De Troyer A.** Discharge frequencies of parasternal intercostal and scalene motor units during breathing in normal and COPD subjects. *Am J Respir Crit Care Med* 153: 622–628, 1996.

14. **Gandevia SC, McKenzie DK, and Plassman BL.** Activation of human respiratory muscles during different voluntary manoeuvres. *J Physiol* 428: 387–403, 1990.

15. **Johnson RL Jr, Hsia CCW, Takeda SI, Wait JL, and Glenny RW.** Efficient design of the diaphragm: distribution of blood flow relative to mechanical advantage. *J Appl Physiol* 93: 925–930, 2002.

16. **Laroche CM, Carroll N, Moxham J, and Green M.** Clinical significance of severe isolated diaphragm weakness. *Am Rev Respir Dis* 138: 862–866, 1988.

17. **Legrand A, Brancatisano A, Decramer M, and De Troyer A.** Rostrocaudal gradient of electrical activation in the parasternal intercostal muscles of the dog. *J Physiol* 495: 247–254, 1996.

18. **Legrand A and De Troyer A.** Spatial distribution of external and internal intercostal activity in dogs. *J Physiol* 518: 291–300, 1999.

19. **Legrand A, Ninane V, and De Troyer A.** Mechanical advantage of sternomastoid and scalene muscles in dogs. *J Appl Physiol* 82: 1517–1522, 1997.

20. **Legrand A, Wilson TA, and De Troyer A.** Rib cage muscle interaction in airway pressure generation. *J Appl Physiol* 85: 198–203, 1998.

21. **Raper AJ, Thompson WT Jr, Shapiro W, and Patterson JL Jr.** Scalene and sternomastoid muscle function. *J Appl Physiol* 21: 497–502, 1966.

22. **Wilson TA and De Troyer A.** Effect of respiratory muscle tension on lung volume. *J Appl Physiol* 73: 2283–2288, 1992.

23. **Wilson TA and De Troyer A.** Respiratory effect of the intercostal muscles in the dog. *J Appl Physiol* 75: 2636–2645, 1993.

24. **Wilson TA, Legrand A, Gevenois PA, and De Troyer A.** Respiratory effects of the external and internal intercostal muscles in humans. *J Physiol* 530: 319–330, 2001.